

## Original Article

Farhad Sadeghi\*, Jose Luis Rodriguez and Craig Bonsignore

# Structure and mechanical properties of a multilayer biomedical shaft tubing: effect of layer composition

<https://doi.org/10.1515/polyeng-2021-0266>

Received September 10, 2021; accepted January 5, 2022;

published online February 11, 2022

**Abstract:** Trilayer polymer tubes were manufactured through an extrusion process using Pebax 6333 and high density polyethylene (HDPE) as outer and inner layer, respectively. A maleic grafted linear low-density polyethylene (LLDPE) was used as the bonding layer or tie-layer. Three types of multilayer tubes were produced: (1) outer layer (Pebax) at 70% of the total wall thickness (WT), (2) outer layer at 90% of WT, and (3) outer layer at 20% of WT. The analysis of mechanical properties showed that the inner layer contributes to strength and rigidity of the tube while the outer layer provides flexibility. Melt rheology behavior for HDPE and Pebax were studied, and HDPE showed a more pronounced shear thinning behavior compared to Pebax. Orientations of the tubes were assessed using Fourier transform infrared spectroscopy (FTIR) and it was found that HDPE layer is more sensitive to molecular orientation when extruded compared to Pebax material. Melting behavior for the tubes was investigated using dynamic scanning calorimetry (DSC). The tubes showed two melting temperatures: one associated with HDPE and one with Pebax. The HDPE peak showed a specific shift to a higher melting point for tubes as a result of molecular orientation during processing. Burst and compression testing were performed on the tubes and results demonstrated that the HDPE-rich extrusion showed the highest burst pressure and compression resistance.

**Keywords:** biomedical; extrusion; multilayer; Pebax; shaft; trilayer.

## 1 Introduction

Catheters are widely used in medical devices in actively used procedures, including stent delivery, drug, contrast injection, imaging guided diagnosis, and ablation [1]. These catheters are generally 300–2000 mm long, including of a combination of single-lumen, multi-lumen (cavity in the tube), or even multilayer shaft tubing. Multilayer tubing combines favorable properties of individual materials in one extrusion, enabling functionality that cannot be attained with a single material. For example, a standard trilayer tubing consists of a high density polyethylene (HDPE) inner, a linear low-density polyethylene (LLDPE) bonding layer, and a Nylon outer layer. An HDPE inner material beneficially allows for a low-friction, lubricious surface for effortless insertion of a guidewire, mandrel, or hypotube. A Nylon (or Pebax) outer material eases thermo-bonding to other Nylon sub-components such as: shaft tubing, balloons, luer, etc. A thin LLDPE middle layer primarily serves to bonding the inner and outer layers together. A standard wall thickness distribution consists of the follow: 20–25% inner, ~5% bonding layer, and 70–75% outer. The combination of these materials provides an ideal tube for catheter maneuverability in the cardiovascular or neurological system with tight radii and complex anatomical pathways.

Polymer coextrusion is used when two or more different polymers need to be combined in a layered formation. Industries such as film packaging, pipe extrusion, and blow molding select appropriate layers to obtain both physical and mechanical properties required. Each layer is selected to meet a certain property, such as gas permeability resistance, tensile strength, abrasion resistance, high clarity, flexibility, tear resistance, and thermal sealing [1]. However, combining different polymers to have an optimized multilayer structure requires melt rheology design and an appropriate extrusion setup to provide a stable flow for each stream and uniform distribution of each polymer circumferentially. To eliminate interfacial instability or layer distortion, polymer selection and layer thickness are crucial steps in making a multilayer

\*Corresponding author: Farhad Sadeghi, Confluent Medical Technologies, 27721 La Paz Road, Laguna Niguel, CA 92677, USA, E-mail: Farhad.Sadeghi@confluentmedical.com

Jose Luis Rodriguez and Craig Bonsignore, Confluent Medical Technologies, 27721 La Paz Road, Laguna Niguel, CA 92677, USA

structure [2,3]. Coextrusion technology has evolved over the last decades, enabling a seven-layer laminates which are now common in the film extrusion industry.

Most thermoplastic polymers can be coextruded together. Pebax (tradename from Arkema) for example, is a polyether block amide (PEBA) that consists of a polyamide and polyether. It is widely used in balloon catheters and offers improved flexibility when compared to Nylon [4]. The polyether segment contributes to elastomeric behavior and creates soft segments, whereas the polyamide contributes to the thermoplastic behavior and forms hard segments [5]. Pebax is a hydrophilic polymer and contains amide groups that make it incompatible with polyolefins such as polyethylene [5]. High density polyethylene is a high strength polyethylene that contributes to stiffness and rigidity. The middle layer or tie-layer is a maleic anhydride modified liner low density polyethylene (M-gr-LLDPE) and used to bond the Pebax to the HDPE. This tie-layer is the thinnest layer, primarily serving a bonding role. The tie-layer contains functional groups (grafted by maleic anhydride) that interact with both polymers bonding them together. The overall mechanical property of the final product is a function of each layer. The thickness of the layers is controlled by the law of mixtures: the summation of tensile strength per unit layer thickness [6]. For example, the following equation applies for tubing with two layers:

$$M = ((t_1 m_1) + (t_2 m_2)) / (t_1 + t_2) \quad (1)$$

where “ $M$ ” is the estimated coextruded film mechanical property, “ $t$ ” is polymer layer thickness, and “ $m$ ” is the mechanical property of the layer.

The molecular structure of Pebax includes soft and hard segments as previously mentioned, where the soft segments are mainly the polyether and hard segments are polyamide crystals. The soft to hard segment ratio plays an important role in controlling the physical and mechanical properties of the tube. Warner et al. [4] investigated balloon surfaces made from Pebax. They observed a distribution of hard segments of polyamide in a circumferential orientation in the balloon body. The hard segments were reported to be  $50 \text{ nm} \pm 20 \text{ nm}$  wide by  $300 \text{ nm} \pm 150 \text{ nm}$  long. They identified that the extrusion process was responsible for hard segment orientation along the axial direction.

HDPE is a widely used in polymer extrusion. The physical and mechanical properties of HDPE in final form such as film, tube, or pipe are strongly related to their microstructure, consisting of two phases: amorphous and crystalline. The crystalline phase is composed of packed folded chains that form lamellae blocks. The lamellae blocks are connected to each other by tie chains [7]. In general, the space between lamellae is amorphous phase

material which does not take part in crystallization of lamellae. Crystalline and amorphous phases, depending on the applied process, could show different arrangements and orientations. Most of the products in their final shape have an oriented structure, and consequently the crystalline and amorphous phases align following a preferred direction. Orientation influences the properties from one direction to another direction [8]. An oriented sample has higher mechanical strength along the orientation direction. This orientation can be calculated and analyzed using infrared spectroscopy [9]. If no orientation is applied, the crystals would grow isotropic and form a spherulite structure with isotropic mechanical properties [10].

Multilayer tubes are increasingly utilized for biomedical applications. There is a great potential in using multilayer tubes in different balloon and catheter applications. It is important to characterize and study the effects of material and layer thickness on physical and mechanical properties of tubes. There are very few studies which cover polymer material properties as they relate to multi-layer extrusions, and these details are typically not shared by commercial producers. This study will investigate the effects of HDPE and Pebax materials and their ratio on the crystalline structure of the extrusion, as well as the related physical and mechanical performance catheter shafts using this composite extrusion.

## 2 Materials and methods, and characterization

Two primary resins were used in this study: HDPE with a melt flow index (MFI) of 0.35 g/10 min at 190 °C/2.16 kg (Marlex 5502 from Chevron Phillips), and Pebax 6333 (a thermoplastic elastomer from Arkema-Biomedical grade). Tie-layer is a grafted-maleic anhydride-LLDPE from Orevac. Viscosity was measured using a Dynisco LCR7000 capillary rheometer at 200 °C. The tubes were produced using a multilayer 12 mm diameter GIMAC coextrusion line. The outer diameter (OD) and inner diameter (ID) of tube were 1.7 and 1.3 mm, respectively. Three types of tubes were produced to the specification shown in Table 1. The percentages presented in Table 1 are extreme for each component and the samples are called “rich in HDPE” and “rich

**Table 1:** Specification of extruded tubes.

Tube name	Total wall thickness (WT) (mm)	Pebax WT (%)	Tie-layer WT (%)	HDPE layer WT (%)
Nominal	0.2	70	5	25
Rich in Pebax	0.2	90	5	5
Rich in HDPE	0.2	15	5	80

in Pebax”, respectively. Coextrusion is a sensitive process and viscosities must match for the layers to obtain a uniform part. It has been shown that interfacial instability is observed at a critical wall shear stress that depends on the total flow rate and ratio of each individual layer [11].

DMA (dynamic mechanical analyzer) tests were performed using a DMA 8000 from Perkin Elmer (Waltham, MA) in tension mode. To evaluate orientation and characterize phase formation, FTIR experiments were carried out by recording infrared spectra on a Frontier FTIR instrument from Perkin Elmer (Waltham, MA) with a resolution of  $4\text{ cm}^{-1}$  and an accumulation of 16 scans. The beam was polarized by means of a Spectra-Tech zinc selenide wire grid polarizer. Thermal properties of the films were analyzed using a differential scanning calorimeter (DSC) 6000 from Perkin Elmer. The samples were heated from  $-30$  to  $200\text{ }^{\circ}\text{C}$  at a heating rate of  $10\text{ }^{\circ}\text{C}/\text{min}$ , then cooled at the same rate to  $-30\text{ }^{\circ}\text{C}$  and heated again to  $200\text{ }^{\circ}\text{C}$ . Tensile tests were performed using a Shimadzu (AGS-X series) machine (Kyoto, Japan). The tests were performed per ISO 10555-1 with 25 mm clamp gap and 500 mm/min stretching speed. Burst and compression tests were performed using Pressure Tester (PT-3070) from Confluent Medical Technologies.

Burst test were performed in a water bath and per biomedical norm where tubes were pressurized in a stepwise trend (1 atm increment) with 1.7 atm/s rate and 6 s settling time in between steps until burst occurred. A compression test is opposite to burst, and it is a significant test when tubes are pressurized from outside (an external component like a balloon pushes against the tube/shaft). For this test, the tube is subjected to an external pressure in a using the same conditions as for pressurization above (burst), until a collapse (crush) occurs. Both these tests were performed in  $37\text{ }^{\circ}\text{C}$  water (equivalent to the average human body temperature).

### 3 Results and discussion

The viscosity curves (viscosity versus shear rate at  $200\text{ }^{\circ}\text{C}$ ) for HDPE and Pebax are plotted in Figure 1. HDPE and Pebax are categorized as *thermoplastics*, meaning that their melt viscosity depends on the shear rate applied [10]. The polymer viscosities are important criterion for the coextrusion process. The flow rate of each polymer layer correlates with pressure applied at the die and viscosity of material. The pressure at the die determines the consistency and stability of the melt flow and is important as it maintains the dimensions for the extruded tube [12]. An important factor for polymer coextrusion is the viscosity match between components.

Pebax exhibits a Newtonian plateau in the terminal zone (lower shear rate region). However, the plateau region is less pronounced for HDPE where it shows a higher viscosity and an earlier shear thinning (viscosity reduction with applied shear). This reduction of viscosity in the shear thinning region is due to the molecular alignments and disentanglements of the long polymer chains [10]. The extrusion process for tube is usually designed for a shear

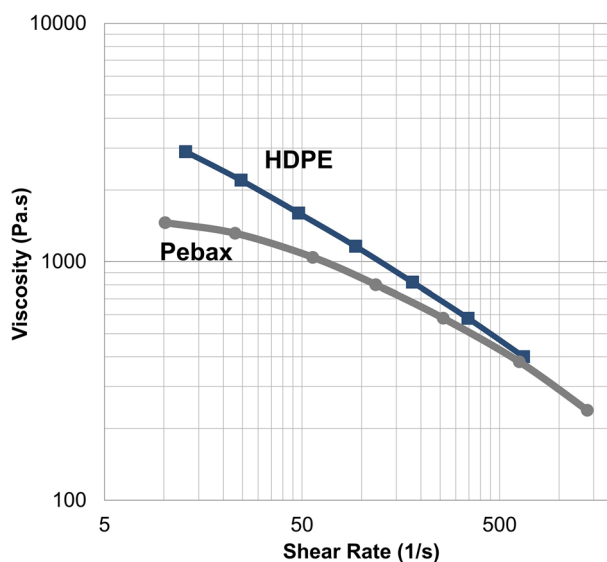


Figure 1: Viscosity curve for HDPE and Pebax at  $200\text{ }^{\circ}\text{C}$ .

rate range of  $100\text{--}1000\text{ s}^{-1}$  [12]. For this study, the range is between  $500$  and  $750\text{ s}^{-1}$  at the die. It is observed that the viscosity is very comparable for two materials at this shear rate range, and it is around  $400\text{ Pa}\cdot\text{s}$ . In the case of a viscosity mismatch, layer distortion can occur, resulting in a disruption during the extrusion process.

In the extrusion process, materials are melted and then enter a water bath where they crystallize and form a morphology. The morphology and orientation within each tube determines the physical and mechanical properties. For this specific tube, the Pebax forms the outer layer and HDPE forms the inner layer. The cross-section and layer arrangements for nominal tube are shown in Figure 2. Pebax constitutes over 70% of the thickness as the outer layer, and HDPE constitutes 25% inner layer, with a tie-layer at 5% of the total wall thickness.

The morphology of Pebax consists of crystallized polyamide (PA) hard segments dispersed in polyether (also called polyethylene oxide-PEO) and amorphous phases of PA (non-crystallized). Armstrong et al. [13] reported a

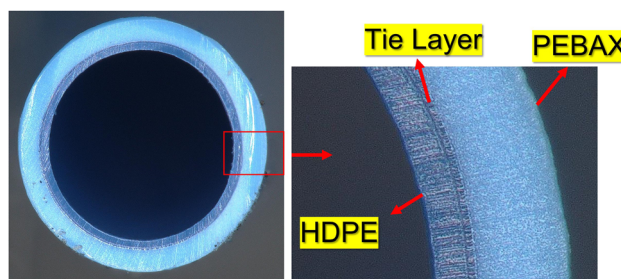
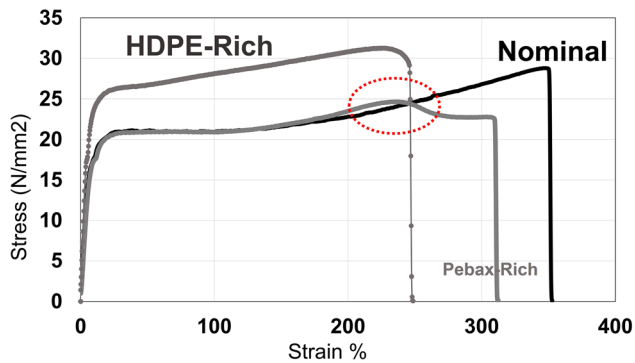


Figure 2: Optical microscopy of the cross-section of the nominal tube.



**Figure 3:** Stress–strain curve of the nominal, HDPE-rich, and Pebax-rich tube samples.

crystallinity of 10.7% for the PEO portion. Sheth et al. [14] reported that Pebax 6333 is composed of 63% Nylon 12 (mol%) and 37% PEO (mol%). HDPE is a highly crystalline polymer with reported crystallinity of about 70% [15].

The tube was extruded through a die before it enters the water bath for cooling and crystallization. Polymer molecules are oriented because of the draw down ratio applied on the extrudate. Orientation of the polymer, either in crystal or amorphous phase, improves mechanical strength. Stretching orients both crystal and amorphous phases, which in turn results in desirable improvements to strength. Sadeghi et al. [8] showed that both the physical and mechanical properties significantly increased with higher orientation. Tensile tests along the tubes were performed, and stress–strain curves are presented in Figure 3. It is observed that the sample rich in HDPE shows the most favorable mechanical properties (greatest yield strength). The necking process is less pronounced for this sample, likely due to lamellar crystal orientation [10]. The nominal sample shows a similar trend to the Pebax rich sample,

with higher strain at break that is likely due to strong bonding between two layers. For the sample rich in Pebax, a delamination in layers occurs, with first portion of curve behaving similar to the nominal sample. Delamination occurs at failure point in the HDPE rich sample.

Strain hardening is observed for all three samples mostly because of a breakdown of initial crystalline structures and formation of fibrillar crystals [8]. In such a process, a saturation in orientation of amorphous phases during stretching is created [8].

Flexibility and stiffness of the tubes are important in their applications. The DMA (dynamic mechanical analyzer) was used to evaluate the tubes stiffness in this study. Figure 4(a) compares the storage modulus ( $E'$ ) and  $\tan(\delta)$  for the nominal, HDPE-rich, and Pebax-rich tube. A smaller storage modulus equates to less stiffness. This can be seen in the Pebax-rich tube and mainly attributed to the presence of the soft segments [14]. HDPE is shown to demonstrate three peaks in DMA testing with increasing temperature corresponding to relaxation mechanisms referred to as  $\alpha$ ,  $\beta$  and  $\gamma$  [16]. The  $\beta$  and  $\gamma$  relaxations correspond to molecular chain movement in the amorphous phase and the  $\alpha$  relaxation is related to chain movement in the crystalline phase. The  $\gamma$  relaxation is normally taken to define the glass transition temperature [16], which is in range of  $-80$  to  $-100$  °C. The next transition is  $\beta$  that is not present here but  $\alpha$  transition is pronounced as it is observed in Figure 4(b). This peak increases linearly with crystallinity for polyethylene and since HDPE has the highest crystallinity, this peak becomes very pronounced. The height and area under  $\tan \delta$  curve indicate the amount of energy that can be absorbed by the sample. A large area under the  $\tan \delta$  curve indicates a greater degree of molecular mobility, which translates into better dampening properties for the HDPE-rich sample [16]. This means that the HDPE-rich sample can better absorb and dissipate

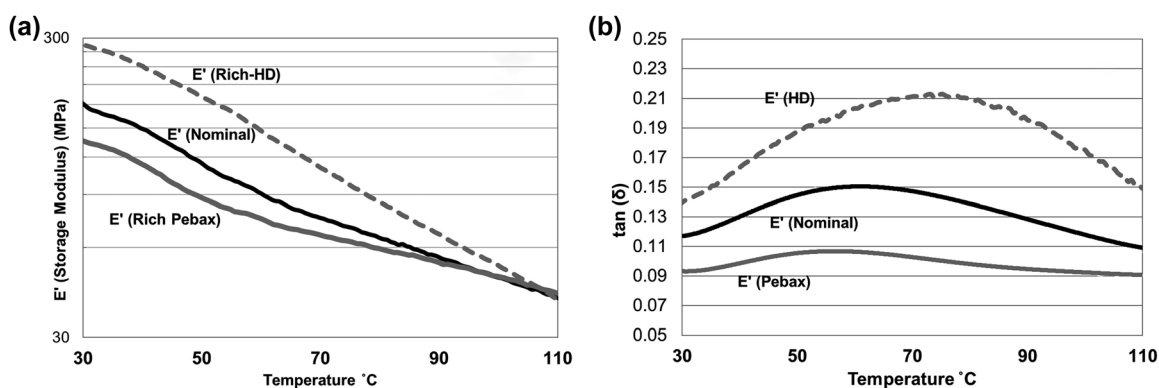


**Figure 4:** DMA results (a) storage modulus ( $E'$ ) (b)  $\tan(\delta)$ .



energy at temperature around 75 °C. However, the Pebax-rich sample shows a transition at lower temperature which translates to a sample that is more flexible with more favorable elastic properties.

Increasing  $\tan(\delta)$  indicates that the material has more energy dissipation potential: the dissipative properties of the material improve with increasing  $\tan(\delta)$ . On the other hand, a decreasing  $\tan(\delta)$  corresponds to more elasticity in the material; thus the material has an increased potential to store an applied load rather than dissipate it. Figure 4(a) shows that HDPE-rich tubes are stiffer than Pebax-rich tubes at room temperature, but increasing temperatures results in decreasing stiffness. The temperature of  $\alpha$  transition is around 51 °C for Pebax-rich sample, coincident with a drop in elastic modulus, and maximum in  $\tan(\delta)$ . In other words, the Pebax-rich tube absorbs the highest energy at this temperature. For the HDPE-rich tube as it is shown in Figure 4(b) that  $T_\alpha$  peak shifts to a higher temperature (76 °C). This is most likely due to the crystalline structure of HDPE that was previously discussed [15].

Dynamic scanning calorimetry (DSC) was used to analyze the thermal behavior of the samples and the results have been shown in Figure 5(a)–(c).

The first heat for the nominal sample (Figure 5(a)), reveals two distinctive melting peaks: one associated with the HDPE layer at 128 °C and one associated with Pebax at 167 °C. Both correspond to the melting temperature of the constituents. The presence of  $T_\alpha$  (at 59 °C) for the nominal tube was observed confirming the DMA results (Figure 4(b)). This peak shifts to lower temperature (50.5 °C) for Pebax-rich tube as shown in Figure 5(a). This is in accordance with data presented in Figure 4(b). The effect of second heating cycle has been shown in Figure 5(b), where the sample was fully melted and crystallized in a quiescent state, erasing its initial orientation history. The comparison between the first heat (tube as it is) and second heat shows a most pronounced effect on HDPE melting peak where the shift in peak implies a higher degree of orientation for this layer in tube structure [8]. This shows that under same processing conditions, the HDPE molecules tends to orient more and form crystals with more defined orientation, whereas Pebax melting peak is not sensitive to orientation (see the orientation calculation in the next section). The DSC of crystallization from the melt reveals a faster and sharper crystallization for Pebax layer than HDPE (Figure 5(c)), with a 27 °C difference in crystallization temperature ( $T_c$ ) observed between the two materials. Increasing the Pebax concentration (Pebax-rich sample) does not displace the crystallization peaks, confirming that the crystallization peaks are independent of their concentration in tube. The delay in crystallization

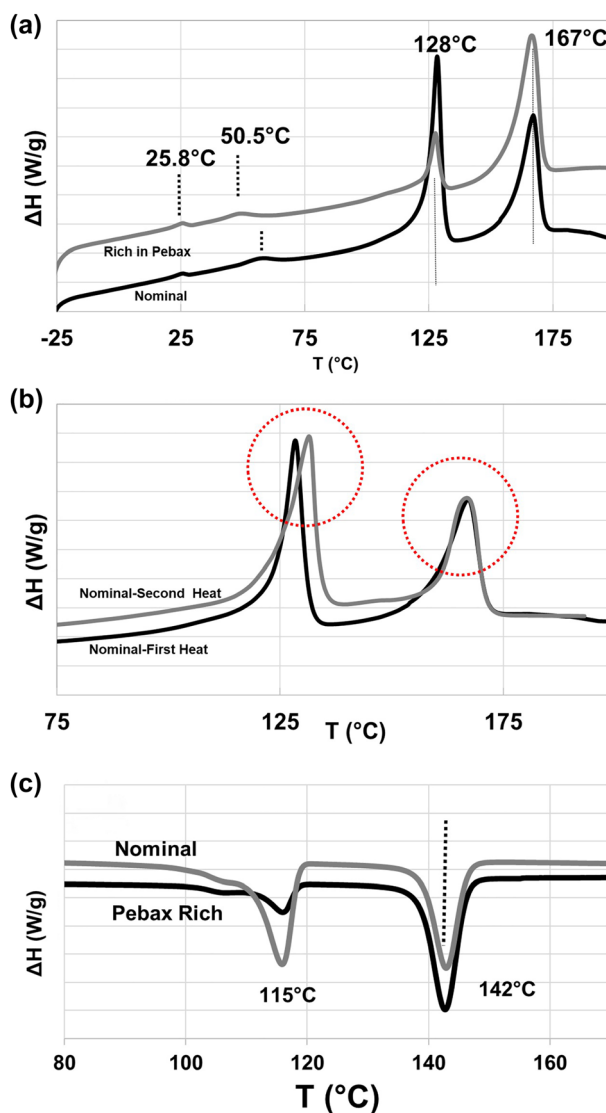


**Figure 5:** DSC results (a) first heat, (b) second heat, (c) cooling crystallization.

for HDPE versus Pebax is likely due to the presence of longer molecular weight polyethylene chains that hinders mobility [16].

FTIR spectroscopy was used to characterize the orientation and phase structure of the samples [17]. Measurements were performed along axial (0°) and radial (90°) directions to evaluate the effect of orientation using a polarized beam. Results are based on the analysis of the energy of different molecular vibration modes associated with specific groups in the molecules. FTIR spectrums are presented in Figure 6 for outer and inner layer, respectively. If there is no orientation, the spectrum at 0- and 90-degrees should have similar adsorption. However, with orientation of molecules, there will be a difference in

intensity and especially the area under the peaks for 0- and 90-degrees spectrum. The first step in orientation calculation is peak selection for each material. In a study by Cole et al., a list of peaks assigned to the different conformations has been proposed for polyamides. These peaks are applicable for Pebax because the hard segments in Pebax are primarily polyamide. Based on the reviewed literature [18] and the experiments executed, three peaks at wave numbers of 904, 936, and 946  $\text{cm}^{-1}$  were selected for FTIR characterizations. The crystals in Pebax tubes mostly consist of  $\alpha$  and  $\gamma$  phases, where  $\alpha$  phase ratio is higher. The peaks at 904 and 946  $\text{cm}^{-1}$  correspond to the  $\gamma$ -crystalline phase, and the 936  $\text{cm}^{-1}$  peak is associated with the  $\alpha$ -crystalline phase of the polyamide. HDPE crystalline orientation can be calculated from two absorptions at 720 and 730  $\text{cm}^{-1}$  corresponding to the b and a crystalline axis, respectively [19].

It is observed in Figure 6 that the Pebax layer is less sensitive to orientation of crystals relative to the HDPE layer. The difference between the 0 and 90° polarized spectrum is much more significant for HDPE layer. This can be revealed through the difference in the area under the peaks for the spectrum at angles of 0 and 90° where the difference for Pebax is insignificant. The higher orientation for HDPE crystals could be related to its higher crystallinity and molecular arrangement structure [16] that was discussed in previous section, and demonstrated in Figure 6b. The orientation calculation and schematic of HDPE layer for three crystalline axes are shown in Figure 7. That is comparable with results obtained by Sadeghi et al. [20] and Bafna et al. [21] where an orientation factor around 0.4 was

reported for extruded HDPE film. The Herman orientation function (f) is used to describe the orientation of given molecular axis with respect to the sample direction [10] in crystal phase and is calculated based on formula discussed by Sadeghi et al. [10]. As it is seen in Figure 7, a uniaxial orientation along machine direction for c axis is observed. However, for the a and b axis, a biaxial (planar) orientation is observed with respect to machine direction.

Burst pressure is an important parameter test parameter in Biomedical applications that represents the strength of tubes and catheters when pressurized [22]. A compression test is opposite to burst, and it is important when tubes are pressurized from outside (an external component like a balloon pushes against the tube/shaft). The results for these two tests are shown in Figure 8. The sample rich in HDPE shows the highest burst pressure and compression resistance. It is very important to note that burst results are in accordance with elastic modulus calculated from tensile results (Figure 3). However, the effect of increasing of HDPE concentration (HDPE rich) on crush resistance improvement is not as significant as burst.

Burst pressure in biomedical application is usually performed in stepwise sequence as described above, with a ramp step and settling time. To evaluate the effect of continuous pressurization without relaxation, a separate test was designed, using a fill rate to achieve a deformation rate similar to that experienced during a tensile test (0.03 ml/s). The nominal tubes were tested for burst and compression test based on such method and results are presented in Figure 9. This test was mainly designed to simulate a tensile test and assess the tube resistance to

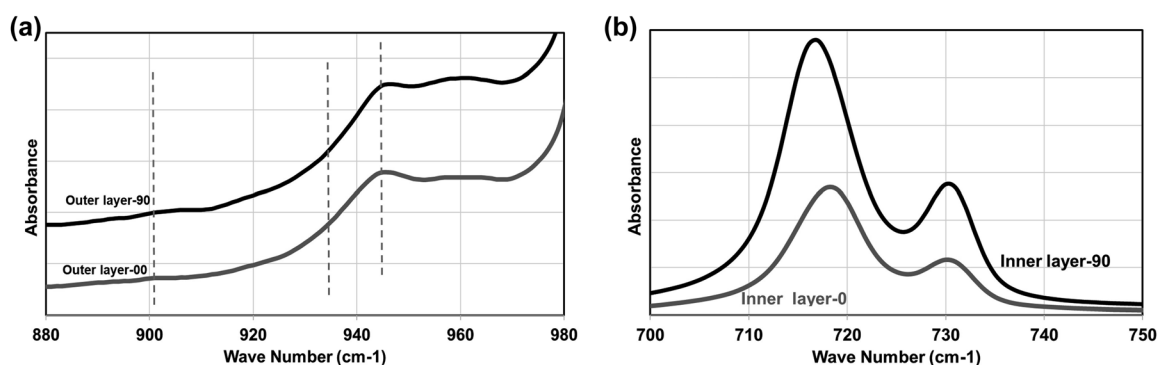


Figure 6: FTIR spectrum of the trilayer tube: outer layer (Pebax) (a) and inner layer HDPE (b).

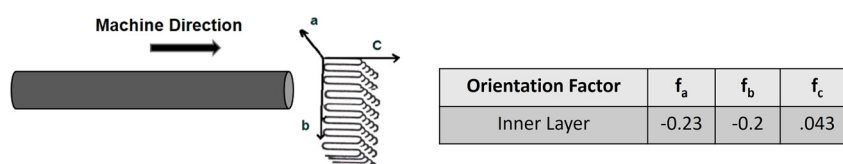


Figure 7: Orientation of crystal lamella.

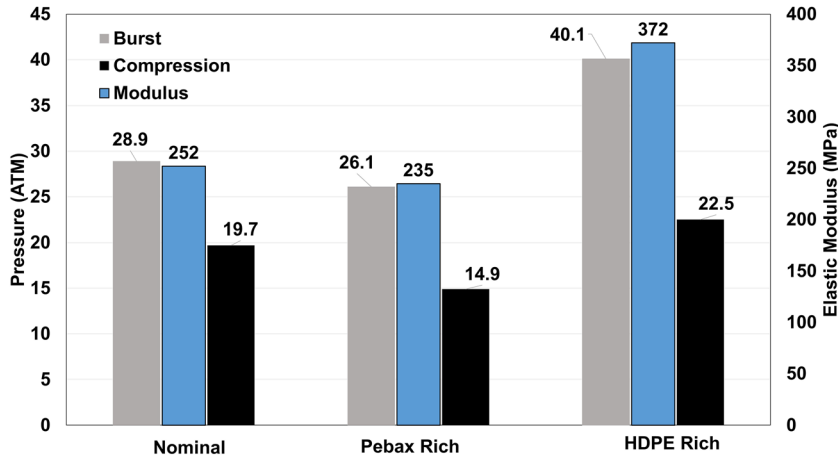


Figure 8: Burst/compression test results.

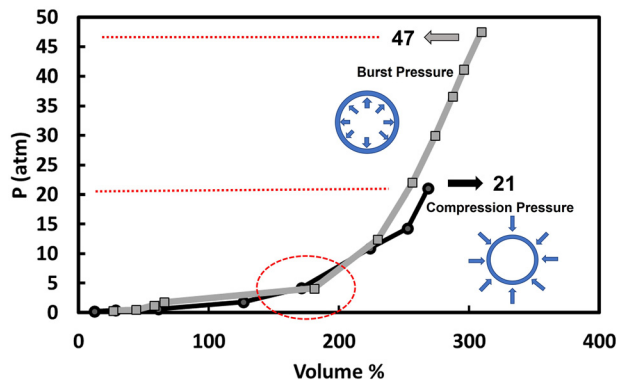


Figure 9: Burst/crush test results in a ramp method for nominal tube.

volume deformation. As it is shown in Figure 9, both curves demonstrate yield at approximately 180% volume deformation. These curves are similar to a tensile curve considering the first portion of the curve as elastic region. The resistance to pressure (slope) increases significantly beyond 180% volume change, This corresponds to the strain hardening section of the tensile curve (see Figure 3). It has been reported that burst pressure of the tube catheter can be calculated based on following formula [23].

$$P = \frac{T(d_o^2 - d_i^2)}{d_i^2 \left(1 + \frac{d_o^2}{d_i^2}\right)} \quad (2)$$

" $T$ " is the tensile strength of the tube, " $d_o$ " is the outer diameter, " $d_i$ " is the inner diameter of the tube, and " $P$ " is the burst pressure of the tube/catheter. Based on this formula, a burst pressure of 57 atm should be obtained for the nominal tube. A difference of 10 atm is observed between the theoretical value and actual number (reported in Figure 9). This is most likely because of burst pressure was performed at body temperature (37 °C) instead of room

temperature. The tensile strength decreases with temperature for polymer. It is important to note that burst pressure in this type of test method (ramp) is more than twice of compression pressure resistance. This could be related to higher tensile to compression strength ratio of part. A higher resistance to tensile versus compression is observed for high density polyethylene when strain rate greater than  $0.04 \text{ s}^{-1}$  is applied [24]. The strain rate applied for the testing of the nominal sample is  $0.30 \text{ s}^{-1}$  that is well above 0.04 limit. In such a strain rate range, the resistance response is stronger in tensile mode compared to compression, which explains a greater burst pressure than compression.

## 4 Conclusions

Tubes from HDPE and Pebax were produced using an extrusion process. The melt rheology and crystalline structure of the tubes were evaluated using DMA, DSC, and FTIR measurements. The physical and mechanical properties of the tube were also studied. Our findings can be summarized as follows:

Three type of tube samples were extruded in various layer concentrations. The sample with highest HDPE concentration showed the maximum tensile properties. The nominal condition, 70% Pebax and 30% HDPE, behaved similarly to the sample with 90% Pebax and 10% HDPE. In these descriptions, the 5% tie layer is included in the HDPE layer ratio. The results were corroborated with DMA tests. HDPE-rich tubes are stiffer than Pebax-rich tubes at room temperature; but as temperature increases the stiffness decreases. Temperature of  $\alpha$  transition is around 51 °C for Pebax-rich sample whereas for HDPE-rich tubes  $\alpha$  peak shifts to a higher temperature (around 76 °C). This is most likely due to the crystalline structure of HDPE. DSC and

FTIR results demonstrate that the HDPE layer is more sensitive to orientation than Pebax layer. The orientation of the HDPE layer is significant and is calculated to about 0.4. The sample rich in HDPE shows the highest burst and compression resistance. The burst results are in accordance with elastic modulus calculated from tensile results. However, the effect of an increasing HDPE concentration ratio did not result in significant improvement of compression resistance compared to burst pressure.

**Acknowledgments:** The authors wish to thank Sayeh Ghaziyani for assisting in plotting the graphs.

**Author contribution:** All the authors have accepted responsibility for the entire content of this submitted manuscript and approved submission.

**Research funding:** None declared.

**Conflict of interest statement:** The authors declare no conflicts of interest regarding this article.

## References

1. Cho S., Lee E., Jo S., Kim G., Woojin K. Extrusion characteristics of thin-walled tubes for catheters using thermoplastic elastomer. *Polymers* 2020, 12, 1628.
2. Karagiannis A., Mavridis H., Hrymak A. N., Vlachopoulos J. *Interface Determination in Multilayer Extrusion*; TAPPI PL&C: Atlanta, GA, 1987; p. 71.
3. Dooley J., Hyun K. S., Hughes K. An experimental study on the effect of polymer viscoelasticity on layer rearrangement in coextruded structures. *Polym. Eng. Sci.* 1998, 38, 1060–1071.
4. Warner J. A., Forsyth B., Zhou F., Myers J., Frethem C., Haugstad G. Characterization of Pebax angioplasty balloon surfaces with AFM, SEM, TEM, and SAXS. *J. Biomed. Mater. Res. B Appl. Biomater.* 2016, 104B, 470–475.
5. Eustache R. P. *Handbook of Condensation Thermoplastic Elastomers: Poly(Ether -b-Amide) TPE, Structure, Properties and Application*; John Wiley & Sons: Weinheim, Germany, 2006.
6. Wagner J. R. *Multilayer Flexible Packaging*, 2nd ed.; Plastics Design Library, Elsevier Inc.: Oxford, UK, Vol. 17, 2016; pp. 281–310.
7. Dasari A., Duncan S. J., Misra R. D. K. Microstructural aspects of tensile deformation of high-density polyethylene. *Mater. Sci. Technol.* 2003, 19, 244–252.
8. Carreau P. J., Sadeghi F. Properties of uniaxially stretched polypropylene films. *Can. J. Chem. Eng.* 2008, 86, 1103–1110.
9. Ajji A., Elkoun S., Huneault M. A., Zhang X. M. Oriented structure and anisotropy properties of polymer blown films: HDPE, LLDPE and LDPE. *Polymer* 2004, 45, 217–229.
10. Ajji A., Carreau P. J., Sadeghi F. J. Study of polypropylene morphology obtained from blown and cast film processes. *J. Plastic Film Sheeting* 2005, 21, 199–217.
11. Han C. D., Shetty R. Studies on multilayer film coextrusion II. Interfacial instability in flat film coextrusion. *Polym. Eng. Sci.* 1978, 18, 180.
12. Giles H. F. Jr., Wagner J. R. Jr., Mount E. M. *The Definitive Processing Guide and Handbook*; Elsevier Science: Chicago, USA, 2013.
13. Armstrong S., Freeman B., Hiltner A., Baer E. Gas permeability of melt-processed poly(ether block amide) copolymers and the effects of orientation. *Polymer* 2012, 53, 1383–1392.
14. Sheth J. P., Wilkes G. L., Xu J. Solid state structure–property behavior of semicrystalline poly(ether block amide) PEBAX thermoplastic elastomers. *Polymer* 2003, 44, 743–756.
15. Lagarona M. J., Lopez-Quintana S., Rodriguez-Cabello J. C., Merinoa J. C., Pastor J. M. Comparative study of the crystalline morphology present in isotropic and uniaxially stretched “conventional” and metallocene polyethylene. *Polymer* 2000, 41, 2999–3010.
16. McShane G. J., Mohagheghian I., Stronge W. J. Impact perforation of monolithic polyethylene plates. *Int. J. Impact Eng.* 2015, 80, 162–176.
17. Cole K. C., Depecker C., Jutingy M., Lefebvre J. M., Krawczak P. Biaxial deformation of polyamide-6. *Polym. Eng. Sci.* 2004, 44, 231–240.
18. Rhee S., White J. L. Crystal structure and morphology of biaxially oriented polyamide 12 films. *J. Polym. Sci. B Polym. Phys.* 2002, 40, 1189–1200.
19. Ajji A., Zhang X., Elkoun S. Biaxial orientation in LLDPE films: comparison of infrared spectroscopy, X-ray pole figures, and birefringence techniques. *Polym. Eng. Sci.* 2006, 46, 1182–1189.
20. Ajji A., Sadeghi F. Structure, mechanical and barrier properties of uniaxially stretched multilayer nylon/clay nanocomposite films. *Int. Polym. Process.* 2012, 5, 565–573.
21. Bafna A., McFaddin D., Beaucage G., Merrick-Mack J., Mirabella F. M. Integrated mechanism for the morphological structure development in HDPE melt-blown and machine-direction-oriented films. *J. Polym. Sci. Part B: Polymer* 2007, 45, 1834–1844.
22. Li X. Y., Liu G. Z., Lu C. I., Xu Lx., Zhen L. Internal structure changes of nylon 12 in balloon forming process. *Appl. Mech. Mater.* 2014, 528, 153–161.
23. Ajay P. *Plastics in Medical Devices for Cardiovascular Applications*; William Andrew: Chadds Ford, PA, USA, 2017.
24. Elleuch R., Taktak W. Viscoelastic behavior of HDPE polymer using tensile and compressive loading. *J. Mater. Eng. Perform.* 2006, 15, 111–116.